# A global test of Allen's rule in rodents

Bader Alhajeri, Yoan Fourcade, Nathan Upham, Hasan Alhaddad

RUNNING HEAD: ALLEN'S RULE IN RODENTS

# A GLOBAL TEST OF ALLEN'S RULE IN RODENTS

BADER H. ALHAJERI[1,†,*], YOAN FOURCADE[2,†], NATHAN S. UPHAM[3,4], HASAN ALHADDAD[1],

[1]*Department of Biological Sciences, Kuwait University, Safat, 13060, Kuwait*

[2]*Sorbonne Université, UPEC, CNRS, IRD, INRAE, Institut d'écologie et des sciences de l'environnement, IEES, F-75005 Paris, France*

[3]*Department of Ecology and Evolutionary Biology, Yale University, New Haven, CT, 06511, USA*

[4]*School of Life Sciences, Arizona State University, Tempe, AZ, 85287, USA*

[†]BHA and YF contributed equally to this work and should be considered as co-first author.

**Corresponding author*: Bader H. Alhajeri (bader.alhajeri@ku.edu.kw)

## ACKNOWLEDGMENTS

The authors did not receive any specific financial support for this work. NSU was supported by NSF grant DEB-1441737 and the Biodiversity Knowledge Integration Center at Arizona State University. Some of the morphometric data used in this study were collected by A. Almousawi, M. Alkhudher, F. Almousa, and Z. Almousawi as part of student-led projects under the supervision of BHA and HA. This work relied on data from IUCN, WorldClim, museum databases, and the literature, and as such, we are grateful to everyone who contributed to these sources. This manuscript improved by comments from S. Meiri, M. Symonds, and two anonymous reviewers.

## FUNDING

The authors did not receive any specific grant funding for this project.

## AUTHOR CONTRIBUTIONS

BHA conceived and designed the study and wrote the first draft of the manuscript. BHA, YF, NSU, and HA collected the data. BHA, YF, and NSU ran preliminary analyses. YF ran all the final analyses and produced the figures. BHA and YF wrote the final version of the manuscript with input from NSU and HA. All authors read and approved the final manuscript.

## BIOSKETCH

**BADER H. ALHAJERI** is an Associate Professor of Zoology in the Department of Biological Sciences at Kuwait University. He is interested generally in mammalian evolutionary ecology, and particularly the macroecological causes of morphological variation among species, at very broad spatial and taxonomic scales. Most of his research uses rodents as the study system. More information can be found on his website: https://sites.google.com/view/alhajeri.

**YOAN FOURCADE** is an Assistant Professor at Université Paris Est Créteil and in the Institute of Ecology and Environmental Sciences of Paris. He is broadly interested in conservation biology and spatial ecology. His current research topics deal with the interaction between local and macroecological processes in the context of climate change.

DR. BADER H ALHAJERI (Orcid ID : 0000-0002-4071-0301)
DR. YOAN FOURCADE (Orcid ID : 0000-0003-3820-946X)
DR. NATHAN UPHAM (Orcid ID : 0000-0001-5412-9342)

Article type : Research Papers

# A GLOBAL TEST OF ALLEN'S RULE IN RODENTS

**RUNNING TITLE:** ALLEN'S RULE IN RODENTS

Word count (excluding title, abstract, references, and supplementary material): 6374
Number of references: 87
Number of figures: 3
Number of tables: 0

## Abstract

**Aim:** We test whether geographic variation in length of rodent species' appendages follows predictions of Allen's rule—a positive relationship between appendage length and temperature—at a broad taxonomic scale (order Rodentia). We also test if the applicability of this rule varies based on the unit of analysis (species or assemblage), examined appendage (tail, hind foot, ear), body size, occupied habitat, geographic range size, life mode, and saltation ability.

**Location:** Worldwide.

**Time period:** Current.

**Major taxa studied:** Rodents (order Rodentia).

**Methods:** We assembled data on morphology, ecology, and phylogeny for up to 2,212 rodent species—representing ~86% of all the described rodent species and ~95% of the described genera. We tested the predicted Allen's rule associations among size-corrected appendage lengths and both latitude and climatic variables (temperature and precipitation). We applied a cross-species approach based on phylogenetic regressions and a cross-assemblage approach based on spatial regressions in equal-area 1.5-degree grid cells.

**Results:** Support for Allen's rule was greatest for the tail and was stronger across assemblages than across species. We detected a negative relationship between tail length and (absolute) latitude, which was accounted for by a positive association between tail length and temperature of the coldest month. This association was greatest in desert species. In addition, we observed a negative relationship between ear length and precipitation.

**Main conclusions:** In rodents, Allen's rule is confirmed only for tails, and this association seems to be driven by adaptation to the cold, rather than warm temperatures. Habitat type seems to influence conformity to this rule. Conformity to Allen's rule is likely the result of complex evolutionary trade-offs between temperature regulation and other essential species' traits.

**KEYWORDS**

Allen's rule, body size, ear length, habitat, hind foot length, geographic range, macroecology, rodent, tail length, temperature

## 1 | INTRODUCTION

Allen's (1877) rule posits that the appendages (e.g., limbs, ears, tail, snout) of endotherms tend to be longer and thinner in warmer environments. This rule is among the most studied biogeographic patterns, perhaps second only to Bergmann's (1847) rule, which also makes a prediction about the adaptive response of endothermic animals to climate. These rules are related, and both are commonly interpreted as reoccurring geographic patterns in morphology shaped by adaptation to climate. More specifically, the modification of surface-area-to-volume ratio aids thermoregulation—its decrease in cold environments reduces heat loss and its increase in warm environments facilitates heat dissipation (Mayr, 1956).

Allen's rule has been examined in various endotherms, including birds (e.g., Nudds & Oswald, 2007; Symonds & Tattersall, 2010; McCollin et al., 2015) and mammals (e.g., lagomorphs: Griffing, 1974; Stevenson, 1986; primates: Fooden & Albrecht, 1999; Tilkens et al., 2007; and rodents: Lindsay, 1987; Bidau et al., 2011; Alhajeri, 2016); it has also been examined in ectotherms (e.g., Ray, 1960). So far, most mammal studies of Allen's rule were conducted at the intraspecific level, while cross-species analyses are often restricted to a few species (often within a taxonomically restricted group). However, recent mammal studies have explored the applicability of this rule to broader taxonomic levels (e.g., Gohli & Voje, 2016; Alroy, 2019), following up on earlier large-scale cross-species bird studies (e.g., Nudds & Oswald, 2007;

Symonds & Tattersall, 2010). Furthermore, cross-assemblage investigations of Allen's rule are rare, if they exist at all, even though this approach is commonly used to study other biogeographic trends (e.g., Blackburn & Hawkins, 2004; Olalla-Tárraga et al., 2010; Maestri et al., 2016; Alhajeri et al., 2019). The role of ecological and geographic factors in conformity to this rule is also an understudied topic. Recently, using a sample of 360 New World small mammal species (marsupials, lipotyphlans, rodents), Alroy (2019) found evidence for longer tails in tropical habitats (e.g., rainforests).

Here, we assemble an extensive dataset to test the predictions of Allen's rule globally in Rodentia. Rodents are an outstanding system to study morphological responses to climate at the interspecific level, especially since they comprise >2,000 extant recognized species (Mammal Diversity Database, 2019) (leading to increased statistical power), have near-global geographic distributions (IUCN, 2017) (encountering diverse climates), and vary greatly in body size (Nowak, 1999) (facilitating the study of morphological covariation with climate). We aimed to test whether rodents' appendage lengths (tail, hind foot, ear) vary consistently over geography and climate, and whether Allen's rule can be similarly applied across rodent species as to spatial assemblages of those species. We predict that phenotypes coherent with Allen's rule should be more common in species with smaller geographic ranges because they are subject to a narrower range of environmental conditions in which to adapt (see Alhajeri & Fourcade, 2019; Serrat et al., 2008). We also predict a stronger appendage length – temperature association in smaller-sized species—this is because in mammals, the relative effect of size modification on thermoregulation (through changes in the surface-area to volume ratio) is greater in smaller species, while in larger species, pelage modification plays a larger role in temperature control (see Ashton et al., 2000; Alhajeri & Steppan, 2016; and references therein). Furthermore, based on the results of Alhajeri (2016) and Alroy (2019), we expect Allen's rule to manifest most strongly in rodent tails (compared to the hind foot and the ear), at tropical latitudes, and specifically in deserts. The novelty of the present study stems from the near comprehensive (and global) sampling of rodent species, the tests of influence of ecological factors on conformity to this rule, and the comparison of cross-species vs. cross-assemblage analyses. The broad taxonomic scale employed ensures that most of the covariation between appendage size and temperature is a consequence of evolutionary adaptation via genetic selection (the mechanism implied by most studies of Allen's and Bergmann's rules), rather than phenotypic plasticity.

## 2 | METHODS

### 2.1 | Morphometric data collection

We first compiled a list of all rodent species with range maps available in the International Union for Conservation of Nature (IUCN, 2017). Using this list, we collected external measurement data for all species available in museum databases and the literature. These data consisted of head and body length (total length minus the tail), tail length, hind foot length, and ear length—all in millimeters (mm). We also collected body weight data in grams (g). The following sources contributed most to this database: Arctos, the Collaborative Collection Management Solution (Arctos, 2018; 47,511 observations), VertNet, a Database of Vertebrate Specimen Records (VertNet, 2019; 15,644 observations), the collections database of the Division of Mammals, Smithsonian National Museum of Natural History (NMNH, 2018; 8,445 observations), iDigBio, Integrated Digitized Biocollections (iDigBio, 2019; 6,667 observations), and the database of the zoological collection of the Museum of Comparative Zoology, Harvard University (MCZbase, 2018; 1,113 observations). In total, data was collected from 285 different reference sources, which are listed in Table S1 in the Supporting Information. The museum databases included data from 58 natural history collections (see Table S1).

Our final database consists of measurement data for 81,880 observations, with the number of observations per species ranging from 6,647 (Mus musculus) to several species with a single observation (Table S1). In total, data was collected for 2,212 species (head and body length: n = 2,212; tail length: n = 2,188; hind foot length: n = 2,160; ear length: n = 1,911; body weight: n = 1,191), belonging to 490 genera (Table S2). According to the Mammal Diversity Database (Burgin et al., 2018), the number of rodent species currently described is 2,552, belonging to 513 genera, indicating that we sampled ~86% of the rodent species and ~95% of their genera. Further details about the process of data collection, processing, cleanup, and quality control can be found in Appendix S1. We used our database to calculate the species means (Table S2) and standard deviations for each measurement. Because the length of species' appendages is correlated to their body size, we need to size-correct each measurement. One option is to calculate the relative length of each appendage by dividing it by body length (e.g. Coetzee, 1970; Fooden & Albrecht, 1999; Bidau et al., 2011; Alhajeri, 2016). Appendage lengths could alternatively be size corrected by computing the residuals of regressions of each species

mean appendage value (tail length, hind foot length, ear length) against the species mean value of head and body length (used as an estimate of body size) (e.g., Alroy, 2019). Here, however, we accounted for the relationship between appendage length and body size by including head and body length as an additional predictor in all statistical models (see section 2.3 and 2.4 below) (see Freckleton, 2002).

## 2.2 | Environmental data collection

We extracted distributional data for all 2,212 rodent species from IUCN (2017). These data consist of polygons depicting each species' known global range based on a combination of empirical records, knowledge of elevational and habitat requirements, and expert assessment. Although these range maps may not accurately represent the exact locations where species are present, they are currently the best global assessment of species' distributions at a large taxonomic scale (Schipper et al., 2008). We downloaded IUCN range maps as Environmental Systems Research Institute (Esri) shapefiles from www.iucnredlist.org/resources/spatial-data-download. We kept all polygon subsets, including invasive ranges, as they represent evidence of the adaptation of species to local climates, whether they occur naturally or not. The IUCN shapefiles (polygons) were loaded into R (R Development Core Team, 2019) and manipulated therein using the following libraries: SF (Pebesma, 2018), RGDAL (Bivand et al., 2018), RGEOS (Bivand & Rundel, 2018), and EXACTEXTRACTR (Baston 2020). We used the R library LETSR (Vilela & Villalobos, 2015) to extract the range size of each species (in kilometers squared) based on the IUCN polygons.

In addition, we used the RREDLIST R library (Chamberlain, 2018) to obtain a list of habitats used by each species using the highest hierarchical level of habitat classification in IUCN. We considered all categories of polygons (extant, extinct, introduced) as they represent environmental conditions in which species are able to survive and reproduce, and hence are all representative of their climatic niche. Out of 2,212 species, 1,257 had more than one habitat type in the IUCN classification. In order to reduce habitat to one type only for each species, we downloaded a global map of terrestrial habitats that uses the same IUCN classification (Jung et al, 2020), and extracted the area of all habitat types within each species' range, and then classified these 1,257 species according to the most common habitat. For the remaining 955 species, we kept the habitat type provided by the IUCN red list (Table S2). Several habitat types

are represented by a few species and their inclusion caused multivariate models to crash; therefore, these analyses only included the six main habitat types represented by most species (forest, savanna, shrubland, grassland, rocky areas desert).

Species were divided into one of four life modes which roughly correspond to microhabitat use (arboreal [n=307], scansorial [n=173], subterranean [n=125], terrestrial [n=1565]) (Table S2)—these data were downloaded from www.vertlife.org/data (Wilman et al., 2014; Upham et al., 2020). These life modes are associated with consistent modifications in the appendages that could influence conformity to Allen's rule. A total of 42 species in our dataset did not have life mode data, and thus were not used in multivariate models that use these data.

Saltatorial (i.e., ricochetal) and a semi-saltatorial locomotory modes are associated with consistent modifications to the appendages, which in turn could influence conformity to Allen's rule. The literature was used to assign terrestrial species, based on morphological modifications to saltation, into those that are fully saltatorial, semi-saltatorial, and those with no information on saltation ability (Table S2). The first category (fully saltatorial [n=65]) includes such species as jerboas and kangaroo rats that are extremely specialized for leaping and commonly employ a bipedal hopping gait almost exclusively as their primary mode of locomotion. The second category (semi-saltatorial [n=281]) is much less specialized for leaping (e.g., gerbils and pocket mice) which often use other locomotory modes (e.g., ambulatory or cursorial locomotion), but assume a (quadrupedal) jumping gait on occasion, such as when alarmed to escape predators (i.e., as a secondary mode of locomotion). All other species are included in the third category (no information [n=1866]), which are species for which we could not find any strong evidence in the literature for specialization to saltation (see Table S2 for details).

Allen's rule is commonly explained in terms of the thermoregulation hypothesis, and thus mainly makes predictions about appendage lengths relative to environmental temperature. However, as both temperature and precipitation exhibit strong latitudinal variation, we aimed to disentangle the role of several climate variables in driving the latitudinal patterns in morphological variation. To test which variable contributes to explaining Allen's rule, we used six bioclimatic variables depicting both average annual and maximum and minimum temperature (in °C) and precipitation (in millimeters): BIO1 (annual mean temperature), BIO5 (maximum temperature of the warmest month), BIO6 (minimum temperature of the coldest month), BIO12 (annual precipitation), BIO13 (precipitation of the wettest month), and BIO14 (precipitation of

the driest month) (for details, see Busby, 1991). These bioclimatic variables were downloaded as raster files from WorldClim (version 2), at a resolution of 2.5 arc-min (http://worldclim.org/version2, Fick & Hijmans, 2017), and processed using the R library RASTER (Hijmans, 2017). Version 2 of the WorldClim dataset is based on average temperature and precipitation interpolated from a global database of weather stations, spanning the years 1970 to 2000 (Hijmans, 2017).

Among rodent species, the latitudinal midpoint of geographic ranges — based on the centroid of IUCN range maps — is positively correlated to annual mean temperature (Pearson's $r = 0.743$, $p < 0.050$) and negatively to annual precipitation (Pearson's $r = -0.633$, $p < 0.050$). In addition, high pairwise correlations exist among the temperature variables (Pearson's $r = 0.480$–$0.942$, all $p < 0.050$) and precipitation variables (Pearson's $r = 0.490$–$0.886$, all $p < 0.050$).

## 2.3 | Data analysis

We analyzed the effect of climate on rodents' appendage length both across species and across assemblages. For each type of analysis and for each appendage, we followed the same analytical steps. First, we examined geographical patterns of appendage length by testing the association between appendage length and the absolute value of latitude. Second, we assessed how this pattern could be explained by climatic factors by testing the effect of each of the six bioclimatic variables on the appendage lengths. We selected the best fitting variable among them—the one that leads to the model with the lowest Akaike information criterion score, corrected for small sample size (AICc; Akaike, 1974; Burnham & Anderson, 2002). In all models, we included as explanatory variables both the climate variable to be tested and head and body length to control for the effect of body size on appendage length. An additional null model was computed, excluding climate from the explanatory variables. Third, we computed multivariate models with interactions to test for the effect of various species' characteristics (body size, habitat type, range size, life mode, and saltation ability) on the relationship between appendage length and the selected climate variable.

To account for intraspecific phenotypic variability that may bias comparative analyses across multiple species (Garamszegi & Møller, 2010; Silvestro et al., 2015), we repeated all statistical models 100 times, each time sampling a random value of appendage length and head and body length, following a truncated normal distribution (so that sampled values remain > 0)

with the mean and standard deviation obtained from the observed distribution of values in our database of morphological measurements. Note that for species where measures originated from one single individual, standard deviation = 0 and the same value was sampled at each repetition. Similarly, there may exist large intraspecific variation in the environmental conditions experienced by a species, especially if it is distributed across a large geographical range. To account for this source of uncertainty we also sampled at each iteration, in the cross-species analyses, a random value of the climate variable following a normal distribution with the mean and standard deviation of the observed climate within the species' range.

In all analyses, climate variables, as well as each morphological measurement (tail length, hind foot length, ear length), were scaled and centered to allow post-hoc comparisons of effect sizes (the standardized beta slope coefficients [cross-species: $\beta_{CS}$; cross-assemblage: $\beta_{CA}$]). Appendage lengths, as well as head and body lengths, were also log-transformed before scaling to linearize the relationships and to reduce the influence of outliers. Plots were generated using the R base library and/or the following libraries: GGPLOT2 (Wickham, 2016), PATCHWORK (Pedersen, 2017), VIRIDIS (Garnier, 2018), and GGTREE (Yu et al., 2017). For all analyses, the significance level (p) was set at $\alpha = 0.05$. All 'log' transformation applied in this paper are natural logarithms. Unless otherwise stated, all other analyses and visualizations were carried out using the R base library. Visual inspections of residual plots (residuals vs. predicted values) and Q–Q (quantile-quantile) plots generally lend support to the distributional assumptions of the residuals of all the linear regression models described below. The complete R script used to perform the phylogenetic and spatial regression analyses can be found in Appendix S2.

### 2.3.1 | Cross-species analysis

We first examined the association between appendage length and climate across species, using morphological, geographical, and climatic data obtained at the species-level. From the IUCN range maps, we extracted the mean and standard deviation of the latitudinal coordinates of each species' range. Then, combining range maps with bioclimatic variables (raster files), we extracted for each species the mean and standard deviation of each of the abovementioned six bioclimatic variables across locations of its entire range (for details, see Alhajeri et al., 2015).

Because species are not independent and because there is evidence of phylogenetic conservatism for all studied morphological traits (see Figures 1a, 2a, 3a), we used phylogenetic

regressions to correct for relatedness among species. For this purpose, we used a sample of 100 trees from Upham et al. (2019), the most complete mammalian phylogeny to date. This source had two alternative forms of the phylogenetic trees: (1) 'DNA-only' trees, which only contain the species for which DNA data was available; and (2) 'completed' trees, which also include species missing DNA data that are imputed with birth-death branch lengths within genus- or family-level taxonomic constraints (family if no congeners were sampled for DNA) (for details, see Upham et al., 2019). The reason for analyzing a sample of 100 trees (for both the DNA-only and completed trees) was to consider the uncertainty in phylogenetic placements and node ages.

A total of 98 species in our morphometric data set were not found in Upham et al.'s (2019) trees (Table S3). For these species, we used taxonomic information from both IUCN (2017) and the Integrated Taxonomic Information System (ITIS, 2018) to find synonyms to match the species names from our dataset to those in the phylogenetic tree. We were able to find synonyms for 56 species; the remaining 42 species were not found (Table S3), and thus were not included in the cross-species analyses (but are included in the cross-assemblage analyses; see below). As such, the cross-species analyses are based on 2,170 species for the completed sample of trees and 1,466 species for the DNA-only trees.

We ran phylogenetic regressions with the length of each of the three appendages as response variable and, as explanatory variables, either latitude or one of the six bioclimatic variables, along with the head and body length always included as a covariable (to account for size). Using the selected climatic variable (the one which leads to the lowest AICc), we computed models where explanatory variables were the interactions between climate and: head and body length, habitat type, range size, life mode, saltation ability as well as all main effects. The significance of these interactions was assessed by likelihood-ratio tests comparing a model with and without the interaction. The whole approach was repeated 100 times (because we use a sample of 100 phylogenetic trees) for each of the completed and the DNA-only sample of trees. In addition, for each tree, analyses were repeated 100 times (because we sampled 100 values of morphology and climate), resulting in a total of 540,000 phylogenetic regressions computed (3 appendages [tail, ear, hind foot] × 2 types of phylogenies [DNA-only + completed] × 100 trees × 100 random sampling × 9 sets of variables [latitude + null model + 6 bioclimatic variables + interaction model]).

Phylogenetic linear regressions were computed using the R library PHYLOLM (Ho & Ane, 2014), assuming a Pagel's lambda ($\lambda$) phylogenetic model (Pagel, 1999). Out of 100 trees and 100 sampled values, we report for each climate variable and for the null model the mean AICc weight of the corresponding model. We report the mean estimate of the slope of the relationship between appendage length and climate, and the mean coefficient of interactions between climate and continuous variables across 100 trees and 100 sampled values. For all the above estimates, we also report 95% confidence intervals based on the distribution of these coefficients across the 100 trees and 100 sampled values, as well as the proportion of significantly positive or negative coefficients. Significance of interactions are reported as the proportion of cases with p-value $< 0.05$. Finally, we extracted the mean estimate of the relationship between appendage length and climate (i.e., the selected bioclimatic variable) for each habitat type, life mode and saltation ability.

Phylogenetic trees were loaded into R and manipulated therein using the following libraries: GEIGER (Harmon et al., 2008), TREEIO (Yu, 2019), and PHYTOOLS (Revell, 2012). The latter R library was also used to estimate ancestral values of appendage lengths using a re-rooting maximum-likelihood method implemented in order to visualize trait evolution within rodent phylogeny.

### 2.3.2 | Cross-assemblage analysis

In addition to species-level analyses, we also examined variation in appendage lengths at the level of rodent species assemblages—this entailed considering a summary value of the traits of all rodent species that co-occur in a given location (i.e., assemblage). We define assemblages as 1.5-degree equal-area grid cells globally, following the best practice recommendations of Hurlbert and Jetz (2007). This assemblage-based approach is commonly used to test macroecological patterns (e.g., Meiri, 2011; Maestri et al., 2016; Alhajeri et al., 2019), and can reveal different insights than the species-based approach, such as community assembly in the former and trait evolution in the latter (Feldman & Meiri, 2014). We first converted IUCN range polygons to presence-absence raster maps at 10 arc-min resolution using LETSR, and then aggregated the maps to a resolution of 1.5 degrees (this also had the effect of reducing computation time). A species was considered present in a grid cell if its distribution overlapped any surface of it, ensuring that all 2,212 species (those in Table S2) were included, even those

with a distributional range smaller than the maps' resolution. Using the associated morphological traits, we summarized in each grid cell the tail length, hind foot length, or ear length of all species present in the grid cell, by the median as well as by both the $10^{th}$ and $90^{th}$ percentile length of each appendage (see Alhajeri et al., 2019 for details). We chose the median to obtain a general perspective on species' appendages within an assemblage, without resorting to the mean that may be uninformative in case of highly skewed traits' distributions. In addition, summarizing assemblages by the $10^{th}$ and $90^{th}$ percentile value of appendages' length was necessary to be able to detect an effect of climate if selection acts mostly on species with unusually long or short appendages.

To control for the effects of spatial autocorrelation, we performed spatial regressions with eigenvector spatial filtering. In this procedure, we computed Moran's eigenvectors (Dray et al., 2006) that describe the spatial configuration of the grid cells and included them as additional predictors in the linear regressions. This ensures that the resulting $\beta$ estimates and associated p-values for the variables of interest (here latitude or bioclimatic variables) are free from the effect of spatial autocorrelation. To prevent overfitting, we selected a set of Moran's eigenvectors via forward selection by permutation, according to the following criteria: all Moran's eigenvectors are significant at the 0.05 level, the difference in model $R^2$ with the previous step is higher than 0.005, and the whole set of Moran's eigenvectors does not account for more than 95% of total variation. The calculation of Moran's eigenvectors and the spatial regressions were performed using the SPMORAN R library (Murakami & Griffith, 2019), and their selection was performed using the ADESPATIAL R library (Dray et al, 2020). Because species richness is unequal across assemblages, we included as a weight in the models the number of species in each assemblage.

Spatial regressions were run with either the median, $10^{th}$ percentile, or $90^{th}$ percentile length of each of the three appendages in each grid cell (= assemblages) as the response variable; while in all models, head and body length (median, $10^{th}$ percentile, or $10^{th}$ percentile value to match the response variable) as well as the selected Moran's eigenvectors were used as explanatory variables. Other used explanatory variables were, sequentially, either the average latitude or climate (defined as each of the six bioclimatic variables) of each grid cell. When assessing the effect of species' characteristics on the relationship between appendage length and the selected climate (the one which leads to the model with the lowest AICc), we could not test the effect of species-specific categorical variables such as life mode and saltation ability because

they could not be averaged at the scale of whole assemblages. However, we included the interaction between climate and each of head and body length and range size (averaged within species' assemblages). The interaction between climate and habitat type was also included using the main habitat of each grid cell, based on the IUCN habitat map described above; this was computed as the habitat type that covers the most area in each grid cell, while only retaining grid cells with a habitat type corresponding to the six dominant types described above for the cross-species analysis.

All analyses were repeated 100 times, corresponding to 100 sampled values of morphological measurements. In total, 8,100 spatial regressions were computed (3 appendages [tail, ear, hind foot] × 3 types of assemblage-level summaries [median, $10^{th}$, and $90^{th}$ percentiles] × 100 random samples × 9 sets of variables [latitude + null model + 6 bioclimatic variables + interaction model]). Significance of interactions were tested using analysis of variance (ANOVA) based on type-III (partial) sums of squares as implemented in the CAR library (Fox & Weisberg, 2019). The mean estimate of the relationship between appendage length and climate for each habitat type was extracted using the EMMEANS R library (Lenth, 2020). We report for each coefficient the mean and 95% confidence intervals based on the 100 repetitions, along with the number of significantly positive and negative results.

# 3 | RESULTS

## 3.1 | Latitudinal patterns

Across assemblages, when appendage size was summarized by the median, we detected a clear negative relationship between all appendages' length and absolute latitude, which was strongest for tail length (average $\beta_{CA\ (median)} = -0.509$) and weak for hind foot length and ear length (average $\beta_{CA\ (median)} = -0.197$ and -0.140, respectively; Figure S1; Table S4). This relationship was also detected when using the $10^{th}$ percentile of appendage size, but only for hind foot length and ear length. We found no evidence for any significant latitudinal pattern when considering the $90^{th}$ percentile of appendage size. Across species, we observed a negative relationship between latitude and tail length only (Figure S1; Table S4), although the evidence remains scarce (95% confidence intervals slightly span 0 for completed trees and only ca. 60% of phylogenetic regressions were significant). This relationship was also weaker than across assemblages (average $\beta_{CS\ (DNA\text{-}only)} = -0.060$; average $\beta_{CS\ (completed)} = -0.056$). In all relationships between

appendage length and climatic variables described below, we similarly observed that the standardized effect sizes of regression estimates were of smaller magnitude in cross-species than cross-assemblage analyses.

## 3.2 | Climatic patterns

### 3.2.1 | Tail length

Both cross-assemblage and cross-species analyses found strong support for a positive relationship between tail length and temperature, although the selected variable varied depending on the type of analysis, from BIO6 for cross-species analyses (average $\beta_{CS\ (DNA\text{-}only)} = 0.106$; average $\beta_{CS\ (completed)} = 0.103$) to BIO1 (median and 10$^{th}$ percentile length; average $\beta_{CA\ (median)} = 0.472$; average $\beta_{CA\ (10th\ perc)} = 0.280$) and BIO5 (90$^{th}$ percentile length; average $\beta_{CA\ (90th\ perc)} = 0.106$) for cross-assemblage analyses (Table S5 and Figure 1c-d). In addition to these best fit variables, we observed significant relationships between tail length and BIO1 for cross-species analyses, and with all other temperature variables for the cross-assemblage analyses (except BIO6 that was not significant when using 90$^{th}$ percentile length). Moreover, there was also a positive relationship between tail length and precipitation variables, especially BIO12 and BIO13 in the cross-species analyses. This relationship differed depending on the species' habitat type in all cases (Table S6), although differences between habitats were not constant between analyses. In the cross-species analyses, desert and forest species exhibited the strongest relationship between tail length and BIO6, while shrubland species had the weakest relationship, even negative on average (Figure 1d). In contrast, cross-assemblage analyses pointed to different effects of habitat depending on the type of summary statistics we used, and no clear pattern emerged. The median and the 10$^{th}$ percentile of tail length, which were both mainly determined by BIO1, had the lowest relationship with BIO1 in the forest habitat; the habitats with the strongest relationship differed though (median: rocky areas and grassland; 10$^{th}$ percentile: rocky areas and desert). Using the 90$^{th}$ percentile of tail length, we found that shrubland and savanna exhibited a lower relationship between tail length and BIO5 than that of all other habitats (Figure 1e). Overall, there was no other evidence of interaction with species' traits in the cross-species analyses, since no more than 58% of models showed a significant interaction with life mode or saltation (Table S6). However, we note that marginal slopes indicate a clearly significantly positive relationship between BIO6 and tail length in subterranean and non-saltating species,

while confidence intervals cross 0 in the other species' categories (Figure 1e). In the cross-assemblage analyses, the effect of temperature on tail length increased in assemblages composed of species with a small range and, only for the 90$^{th}$ percentile, in assemblages composed of small-sized species (Figure 1e).

### 3.2.1 | Hind-foot length

There was no evidence of a relationship between hind-foot length and climate in the cross-species analyses, as the null model generally had the lowest AICc (Table S5 and Figure 2b). Cross-assemblage analyses revealed opposite trends depending on the summary statistics (Table S5 and Figure 2b-c). Using the median or 10$^{th}$ percentile of hind-foot length, a temperature variable had the best fit overall (BIO1 and BIO6 respectively), and there was generally a positive relationship between hind-foot length and all bioclimatic variables, temperature and precipitation included. However, temperature had no effect on the 90$^{th}$ percentile of assemblage-level hind-foot length, but we observed a negative correlation with all precipitation variables (BIO12 had the best fit on average). Although the effect of climate alone appeared similar, the effect of range size had an opposite effect on the relationship between the median (positive) and 10$^{th}$ percentile (negative) hindfoot length (Table S6 and Figure 2e). Using the 10$^{th}$ percentile, there was also a negative interaction between BIO6 and body size, and a significant effect of habitat type (Table S6) in which BIO6 and hindfoot length show a reduced relationship in savannas, shrublands, and rocky areas compared to other habitats (Figure 2e).

### 3.2.3 | Ear length

Cross-species variation in ear length appeared to be associated with precipitation, as there was strong support for a negative relationship between ear length and BIO14 (precipitation of the driest month) (average $\beta_{CS\ (completed)} = -0.063$; average $\beta_{CS\ (DNA\text{-}only)} = -0.050$; Figure 3c; Table S5). Cross-assemblage results were largely similar to those observed for hindfoot length (Table S5 and Figure 3): the median or 10$^{th}$ percentile of ear length were mostly determined by BIO1 (average $\beta_{CA\ (median)} = 0.195$) and BIO6 (average $\beta_{CA\ (10th\ perc)} = 0.230$) respectively, and were positively related to both temperature and precipitation variables. In contrast, the 90$^{th}$ percentile of assemblage-level ear length was better explained by precipitation (BIO14, average $\beta_{CA\ (90th\ perc)} = -0.070$) and we observed a negative correlation with all precipitation variables (we note,

434 though, that there is also evidence for a positive relationship with BIO5). There was an effect of
435 habitat type in cross-assemblage analyses only (Table S6), that showed desert habitat to have the
436 lowest relationship between the 90$^{th}$ percentile ear length and precipitation, and the highest
437 relationship between median or the 10$^{th}$ percentile ear length and temperature (Figure 3e).
438

439 ## 4 | DISCUSSION

440 We assembled for this study an unprecedentedly large database of rodents' morphological
441 measurements, which, coupled with up-to-date phylogenetic, climatic, and distributional data,
442 allowed us to investigate variation in appendage size in relation to climate at broader spatial
443 scale and taxonomic level than previous works (see Alroy, 2019 for a recent example). We also
444 accounted for intraspecific variation in morphology and in the climatic conditions encountered
445 across the range, which improves the robustness of our conclusions relative to those based on
446 species averages (Ives et al., 2007; Des Roches et al., 2018). At the global scale of order
447 Rodentia, we observed that Allen's rule seems to apply mostly for tails, as this is the only
448 appendage whose size exhibits relatively strong latitudinal variation and a relationship with
449 temperature in both cross-species and cross-assemblage analyses. Generally, the association
450 between appendage lengths and climate appeared to be more clearly detected among units of
451 assemblages than species. Part of this outcome could be driven by the conservative nature of
452 integrating both phylogenetic uncertainty and intra-specific trait variation in the cross-species
453 approach, the former of which is not considered in cross-assemblage analyses. Alternatively, we
454 hypothesize that stronger effect sizes in the cross-assemblage analyses could be caused by
455 geographically widespread species, which may disproportionally contribute to global
456 morphological gradients. If this were the case, cross-species analyses would provide a better
457 assessment of the true dynamics of Allen's rule; therefore, we will mostly focus our
458 interpretation on results that were consistently supported by both cross-species and cross-
459 assemblage analyses.

460 We found that tail lengths seem to increase toward the equator and with increasing
461 temperature. This result is partly in accordance with the desert rodent study of Alhajeri (2016) in
462 that relative tail length was associated with temperature variables (but not hind-foot length nor
463 ear length). Alroy (2019) also detected an increase in relative tail lengths in small mammals in
464 the tropics (and no increase in the size of hind feet or ears); however, in that study, increased tail

length was not associated with increasing temperature, as our analyses suggest. Furthermore, our cross-species analyses suggest that the variation in tail length is driven by BIO6 (minimum temperature of the coldest month) rather than BIO1 (mean annual temperature) or BIO5 (maximum temperature of the warmest month). This can be explained in terms of this association being adaptive for heat conservation in cold environments (by having relatively shorter tails) rather than heat dissipation in warmer environments (by having relatively longer tails). A similar interpretation was proposed in birds, where appendage size (bill and tarsus lengths) was found to be mostly associated with winter temperature (Nudds & Oswald, 2007; Danner & Greenberg, 2015; Friedman et al., 2017; Fan et al., 2019; Romano et al., 2020). Cold temperatures appear to be a greater evolutionary constraint than warm ones.

We also found evidence that conformity to Allen's rule (in tail length) varies depending on the habitat type—more specifically, a stronger pattern is observed in desert and forest species. For the former, this may indicate that variation in tail length is driven by thermoregulatory pressures. However, it has also been previously suggested (e.g., Alroy, 2019) that the increase in tail lengths with decreasing latitude is caused by increased tropical arboreality. However, we did not find an effect of life mode on the strength of the relationship between tail length and BIO6. Moreover, the greater tail length increase in some deserts (e.g., Sahara, Arabia, central Asia, western Australia, and to a lesser degree Mexico; Figure 1b) could be driven by increased saltatorial ability in such habitats, where a longer tail aids in aerial balance (see Alhajeri, 2016). Thus, convergence toward longer tails could have been driven by extreme selective pressures in desert environments, as is the case in other morphological traits in desert rodents (Mares, 1975; Kotler et al., 1994; Alhajeri et al., 2016; Alhajeri, 2016, 2018; Alhajeri & Steppan, 2018a, b). We could not, however, test the effect of saltation ability at the scale of assemblages, and analyses conducted across species did not show a significant interaction of this variable on the relationship between tail length and temperature, although some results (see Figure 1e) may point to a stronger relationship in non-saltating species, contradicting the hypothesis above.

For the 90$^{th}$ percentile, Allen's rule seems to more strongly apply in assemblages composed of small-sized species, and weakly to assemblages of large-sized species. This could be explained by the fact that a modification in tail length would have a disproportionately stronger effect on the surface-area to volume ratio (and thus thermoregulation) in smaller rodent species (see Introduction). The stronger effect of temperature on tail length in assemblages

composed of small-ranged species could be driven by the fact that these species are subjected to a narrower range of environmental conditions for which to adapt.

In addition, we also observed that the variation of ear length (across species) could be explained by a negative relationship between ear length and the precipitation variable BIO14 (precipitation of driest month). In birds, there is evidence of the opposite (positive) relationship between appendage length and precipitation/humidity. Indeed, longer bills have been found to be associated with higher humidity, a pattern that was attributed to the need of more efficient heat dissipation at high humidity during summer, because humidity reduces evaporative cooling at high temperature (Gardner et al., 2016). Here, a possible explanation for the tendency for ear length to decrease with increasing precipitation could be that this pattern is adaptive in dry and hot environments, where longer appendage sizes help heat dissipation as per the prediction of Allen's rule. In addition, desert habitats had a strongly negative relationship between the 90$^{th}$ percentile ear length and precipitation, which suggests that rodents in the driest desert habitats have the longest ears. Although there is no clear prediction of the role precipitation may have in driving appendage length variation in mammals, our results suggest that such a relationship exists. More thorough investigations of the complex link between inter- or intra-specific variation in appendage size and precipitation, such as non-linear relationships or interactions with temperature, may help to more fully decipher the underlying mechanisms.

In conclusion, Allen's rule is observed at the global scale in rodents but can only be confidently asserted for tails. The length of hind feet shows no relationship with climatic variables in cross-species, phylogenetically informed analyses. The case of ear length is somewhat intermediate: measured across species, it does not show latitudinal variation nor a relationship with temperature, but it appeared to be associated with global variation in precipitation. Furthermore, it seems that certain species characteristics either promote or hinder the observance of this rule, while others have no effect upon it. Therefore, we provide evidence here of a strong departure from the global expectations of Allen's rule, i.e. a general increase in the length of all appendages with increasing temperature. Most likely, this pattern reflects trade-offs between selection for thermoregulation and for alternative traits (locomotion, in the case of tails and hind feet). Additional studies on other taxa, conducted at the same global spatial scale and high taxonomic resolution, would help assess whether conformity to Allen's rule can be

considered a general, widespread pattern, or is a more idiosyncratic pattern restricted to a few species groups and specific appendages.

## DATA ACCESSIBILITY

All data and R code generated in this study are available in the supporting information.

ACKNOWLEDGMENTS -.

FUNDING -.

AUTHOR CONTRIBUTIONS -.

## REFERENCES

Akaike, H. (1974) A new look at the statistical model identification. IEEE Transactions on Automatic Control, 19, 716–723.

Alhajeri, B. H., Hunt, O. J., & Steppan, S. J. (2015). Molecular systematics of gerbils and deomyines (Rodentia: Gerbillinae, Deomyinae) and a test of desert adaptation in the tympanic bulla. Journal of Zoological Systematics and Evolutionary Research, 53, 312–330.

Alhajeri, B. H. (2016). A phylogenetic test of the relationship between saltation and habitat openness in gerbils (Gerbillinae, Rodentia). Mammal Research, 61, 1–11.

Alhajeri, B. H., & Steppan, S. J. (2016). Association between climate and body size in rodents: A phylogenetic test of Bergmann's rule. Mammalian Biology, 81, 219–225.

Alhajeri, B. H. (2018). Craniomandibular variation in the taxonomically problematic gerbil genus Gerbillus (Gerbillinae, Rodentia): Assessing the influence of climate, geography, phylogeny, and size. Journal of Mammalian Evolution, 25, 261–276.

Alhajeri, B. H., & Steppan, S. J. (2018a). A phylogenetic test of adaptation to deserts and aridity in skull and dental morphology across rodents. Journal of Mammalogy, 99, 1197–1216.

Alhajeri, B. H., & Steppan, S. J. (2018b). Community structure in ecological assemblages of desert rodents. Biological Journal of the Linnean Society, 124, 308–318.

Alhajeri, B. H., & Fourcade, Y. (2019). High correlation between species-level environmental data estimates extracted from IUCN expert range maps and from GBIF occurrence data. Journal of Biogeography, 46, 1329–1341.

Alhajeri, B. H., Porto, L. M. V., & Maestri, R. (2019). Habitat productivity is a poor predictor of body size in rodents. Current Zoology, zoz037. https://doi.org/10.1093/cz/zoz037

Allen, J. A. (1877). The influence of physical conditions in the genesis of species. Radical Review, 1, 108–140.

Alroy, J. (2019). Small mammals have big tails in the tropics. Global Ecology and Biogeography, 28, 1042–1050.

Arctos (2018). Arctos, Collaborative Collection Management Solution. Downloaded on 2018 September 18. http://arctos.database.museum

Ashton, K. G., Tracy, M. C., Queiroz, A. (2000). Is Bergmann's Rule Valid for Mammals? The American Naturalist, 156, 390–415.

Daniel Baston. (2020). exactextractr : Fast Extraction from Raster Datasets using Polygons. R package version 0.4.0. https://CRAN.R-project.org/package=exactextractr

Bergmann, C. (1847). Über die Verhältnisse der Wärmeökonomie der Thiere zu ihrer Grösse. Göttinger Studien, 3, 595–708.

Bidau, C., Martí, D., & Medina, A. (2011). A test of Allen's rule in subterranean mammals: The genus Ctenomys (Caviomorpha, Ctenomyidae). Mammalia, 75, 311–320.

Bivand, R., & Rundel, C. (2018). rgeos: Interface to Geometry Engine-Open Source (GEOS). R package version 0.3-28. https://CRAN.R-project.org/package=rgeos

Bivand, R., Keitt, T., & Rowlingson, B. (2018). rgdal: Bindings for the 'Geospatial' Data Abstraction Library. R package version 1.3-3. https://CRAN.R-project.org/package=rgdal

Blackburn, T. M., & Hawkins, B. A. (2004). Bergmann's rule and the mammal fauna of northern North America. Ecography, 27, 715–724.

Blix, A. S., (2016). Adaptations to polar life in mammals and birds. Journal of Experimental Biology, 219, 1093–1105.

Burgin, C. J., Colella, J. P., Kahn, P. L., & Upham, N. S. (2018). How many species of mammals are there? Journal of Mammalogy, 99, 1–14.

Burnham, K. P., & Anderson, D. R. (2002). Model Selection and Multi-Model Inference: A Practical Information-Theoretic Approach. Springer-Verlag, New-York.

Busby, J. R. (1991). BIOCLIM: a bioclimate analysis and prediction system. Plant Protection Quarterly, 61, 8–9.

587 Chamberlain, S. (2018). rredlist: 'IUCN' Red List Client. R package version 0.5.0.
588 https://CRAN.R-project.org/package=rredlist
589 Coetzee, C. G. (1970). The Relative Tail-Length of Striped Mice Rhabdomys pumilio Sparrman
590 1784 in Relation to Climate. Zoologica Africana, 5, 1–6.
591 Danner, R. M., & Greenberg, R. (2015). A critical season approach to Allen's rule: bill size
592 declines with winter temperature in a cold temperate environment. Journal of
593 Biogeography, 42, 114–120.
594 Des Roches, S., Post, D.M., Turley, N.E., Bailey, J.K., Hendry, A.P., Kinnison, M.T.,
595 Schweitzer, J.A. & Palkovacs, E.P. (2018) The ecological importance of intraspecific
596 variation. Nature Ecology & Evolution, 2, 57–64.
597 Dray, S., Legendre, P., & Peres-Neto, P. R. (2006). Spatial modelling: a comprehensive
598 framework for principal coordinate analysis of neighbour matrices (PCNM). Ecological
599 Modelling, 196, 483–493.
600 Dray, S., Blanchet, G., Borcard, D., Guenard, G., Jombart, T., Larocque, G., Legendre, P., &
601 Wagner, H. H. (2020). adespatial: Multivariate Multiscale Spatial Analysis. R package
602 version 0.3-8. https://CRAN.R-project.org/package= adespatial
603 Fan, L., Cai, T., Xiong, Y., Song, G., & Lei, F. (2019). Bergmann's rule and Allen's rule in two
604 passerine birds in China. Avian Research, 10, 34.
605 Feldman, A., & Meiri, S. (2014). Australian Snakes Do Not Follow Bergmann's Rule.
606 Evolutionary Biology, 41, 327–335.
607 Fick, S. E., & Hijmans, R. J. (2017). Worldclim 2: New 1-km spatial resolution climate surfaces
608 for global land areas. International Journal of Climatology, 37, 4302–4315.
609 Fooden, J., & Albrecht, G. H. (1999). Tail-Length Evolution in Fascicularis-Group Macaques
610 (Cercopithecidae: Macaca). International Journal of Primatology, 20, 431–440.
611 Fox, J., & Weisberg, S. (2019). An R Companion to Applied Regression. Third edition. Thousand
612 Oaks, CA: Sage.
613 Freckleton, R.P. (2002) On the misuse of residuals in ecology: Regression of residuals vs.
614 multiple regression. Journal of Animal Ecology, 71, 542–545.
615 Friedman, N. R., Harmácková, L., Economo, E. P., & Remeš, V. (2017). Smaller beaks for
616 colder winters: Thermoregulation drives beak size evolution in Australasian songbirds.
617 Evolution, 71, 2120–2129.

618 Garamszegi, L. Z., & Møller, A. P. (2010). Effects of sample size and intraspecific variation in
619 phylogenetic comparative studies: A meta-analytic review. Biological Reviews, 85,
620 797-805.
621 Gardner, J. L., Symonds, M. R. E., Joseph, L., Ikin, K., Stein, J., & Kruuk, L. E. B. (2016).
622 Spatial variation in avian bill size is associated with humidity in summer among Australian
623 passerines. Climate Change Responses, 3, 11.
624 Garnier, S. (2018). viridis: Default Color Maps from 'matplotlib'. R package version 0.5.1.
625 https://CRAN.R-project.org/package=viridis
626 Gohli, J., & Voje, K.L. (2016). An interspecific assessment of Bergmann's rule in 22
627 mammalian families. BMC Evolutionary Biology, 16, 1–12.
628 Griffing, J. P. (1974). Body measurements of black-tailed jackrabbits of Southeastern New
629 Mexico with implications of Allen's rule. Journal of Mammalogy, 55, 674–678.
630 Wilman, H., Belmaker, J., Simpson, J., de la Rosa, C., Rivadeneira, M. M., & Jetz, W. (2014)
631 EltonTraits 1.0: Species-level foraging attributes of the world's birds and mammals.
632 Ecology, 95, 2027.
633 Harmon, L. J., Weir, J. T., Brock, C. D., Glor, R. E., & Challenger, W. (2008). GEIGER:
634 investigating evolutionary radiations. Bioinformatics, 24, 129–131.
635 Hijmans, R. J. (2017). raster: Geographic Data Analysis and Modeling. R package version 2.2-
636 12. https://CRAN.R-project.org/package=raster
637 Ho, L. S. T., & Ane, C. (2014). A linear-time algorithm for Gaussian and non-Gaussian trait
638 evolution models. Systematic Biology, 63, 397–408.
639 Hurlbert, A. H., & Jetz, W. (2007). Species richness, hotspots, and the scale dependence of range
640 maps in ecology and conservation. Proceedings of the National Academy of Sciences, 104,
641 13384–13389.
642 iDigBio (2019). iDigBio, Integrated Digitized Biocollections. Downloaded on 2019 July 4.
643 https://www.idigbio.org/portal/search
644 ITIS (2019). Integrated Taxonomic Information System. Accessed on 2019 October 6 – 10.
645 http://www.itis.gov
646 IUCN (2017). The IUCN Red List of Threatened Species. Version 3. Downloaded on 2019 June
647 9. https://www.iucnredlist.org

Ives, A.R., Midford, P.E. & Garland, T.J. (2007) Within-species variation and measurement error in phylogenetic comparative methods. Systematic Biology, 56, 252–270.

Jung, M., Dahal, P. R., Butchart, S. H. M., Donald, P. F., De Lamo, X., Lesiv, M., Kapos, V., Rondinini, C., & Visconti, P. (2020). A global map of terrestrial habitat types [Data set]. Zenodo. https://doi.org/10.5281/zenodo.3816946

Kotler, B. P., Brown, J. S., & Mitchell, W. A. (1994). The Role of Predation in Shaping the Behavior, Morphology and Community Organization of Desert Rodents. Australian Journal of Zoology, 42, 449–466.

Lenth, R. (2020). emmeans: Estimated Marginal Means, aka Least-Squares Means. R package version 1.4.6. https://CRAN.R-project.org/package=emmeans

Lindsay, S. L. (1987). Geographic size and non-size variation in Rocky Mountain Tamiasciurus hudsonicus: significance in relation to Allen's rule and vicariant biogeography. Journal of Mammalogy, 68, 39–48.

Maestri, R., Luza, A. L., de Barros, L. D., Hartz, S. M., Ferrari, A., de Freitas, T. R. O., & Duarte, L. D. S. (2016). Geographical variation of body size in sigmodontine rodents depends on both environment and phylogenetic composition of communities. Journal of Biogeography, 43, 1192–1202.

Mainwaring, M. C., & Street, S. E. (2019). Conformity to Bergmann's rule in birds depends on nest design and migration. bioRxiv, 686972. https://doi.org/10.1101/686972

Mammal Diversity Database (2019). American Society of Mammalogists. Accessed on 2019 October 4. www.mammaldiversity.org

Mares, M. A. (1975). South American mammal zoogeography: evidence from convergent evolution in desert rodents. Proceedings of the National Academy of Sciences, 72, 1702–1706.

Mayr, E. (1956). Geographical character gradients and climatic adaptation. Evolution, 10, 105–108.

McCollin, D., Hodgson, J., & Crockett, R. (2015). Do British birds conform to Bergmann's and Allen's rules? An analysis of body size variation with latitude for four species. Bird Study, 62, 404–410.

MCZbase (2018). Museum of Comparative Zoology, Harvard University, Database of the Zoological Collections. Accessed on 2018 July 10 – August 8. https://mczbase.mcz.harvard.edu

Meiri, S. (2011). Bergmann's Rule – what's in a name? Global Ecology and Biogeography, 20, 203–207.

Murakami, D., & Griffith, D. A. (2019). Eigenvector Spatial Filtering for Large Data Sets: Fixed and Random Effects Approaches. Geographical Analysis, 51, 23–49.

NMNH (2018). Smithsonian National Museum of Natural History, the Division of Mammals Collections Database. Downloaded on 2018 October 8. https://collections.nmnh.si.edu/search/mammals

Nowak, R. M. (1999). *Walker's Mammals of the World. 6th Edition.* Baltimore, MA: Johns Hopkins University Press.

Nudds, R. L., & Oswald, S. A. (2007). An interspecific test of Allen's rule: Evolutionary implications for endothermic species. Evolution, 61, 2839–2848.

Olalla-Tárraga, M. A., Bini, L. M., Diniz-Filho, J. A. F., & Rodríguez, M. A. (2010). Cross-species and assemblage-based approaches to Bergmann's rule and the biogeography of body size in Plethodon salamanders of eastern North America. Ecography, 33, 362–368.

Pagel, M. (1999). Inferring the historical patterns of biological evolution. Nature, 401, 877–884.

Pebesma, E. (2018). Simple Features for R: Standardized Support for Spatial Vector Data. The R Journal, 10, 439–446.

Pedersen, T. L. (2017). patchwork: The Composer of ggplots. R package version 0.0.1. https://github.com/thomasp85/patchwork

R Development Core Team (2019). R: A Language and Environment for Statistical Computing. Vienna, Austria: R Foundation for Statistical Computing. 3.5.3. http://www.r-project.org

Ray, C. (1960). The application of Bergmann's and Allen's rules to the poikilotherms. Journal of Morphology, 106, 85–108.

Revell, L. J. (2012). phytools: an R package for phylogenetic comparative biology (and other things). Methods in Ecology and Evolution, 3 217–223.

Romano, A., Séchaud, R. & Roulin, A. (2020) Geographical variation in bill size provides evidence for Allen's rule in a cosmopolitan raptor. Global Ecology and Biogeography, 29, 65–75.

708 Schipper, J., Chanson, J. S., Chiozza, F., Cox, N. A., Hoffmann, M., Katariya, V., … Young, B.
709 E. (2008). The status of the world's land and marine mammals: Diversity, threat, and
710 knowledge. Science, 322, 225–30.
711 Serrat, M. A., King, D. & Lovejoy, C.O. (2008) Temperature regulates limb length in
712 homeotherms by directly modulating cartilage growth. Proceedings of the National
713 Academy of Sciences, 105, 19348–19353.
714 Silvestro, D., Kostikova, A., Litsios, G., Pearman, P. B., & Salamin, N. (2015). Measurement
715 errors should always be incorporated in phylogenetic comparative analysis. Methods in
716 Ecology and Evolution, 6, 340-346.
717 Stevenson, R. D. (1986). Allen's rule in North American rabbits (Sylvilagus) and hares (Lepus) is
718 an exception, not a rule. Journal of Mammalogy, 67, 312–316.
719 Symonds, M. R. E., & Tattersall, G. J. (2010). Geographical variation in bill size across bird
720 species provides evidence for Allen's rule. The American Naturalist, 176, 188–197.
721 Tilkens, M. J., Wall-Scheffler, C., Weaver, T. D., & Steudel-Numbers, K. (2007). The effects of
722 body proportions on thermoregulation: An experimental assessment of Allen's rule. Journal
723 of Human Evolution, 53, 286–291.
724 Upham, N. S., Esselstyn, J. A., & Jetz, W. (2019). Inferring the mammal tree: Species-level sets
725 of phylogenies for questions in ecology, evolution, and conservation. PLOS Biology, 17,
726 e3000494.
727 Upham, N. S., Esselstyn, J. A., & Jetz, W. (2020) Ecological causes of uneven speciation and
728 species richness in mammals. bioRxiv, 504803.
729 VertNet (2019). VertNet, a Database of Vertebrate Specimen Records. Downloaded on 2019
730 June 29. http://portal.vertnet.org/search
731 Vilela, B., & Villalobos, F. (2015). letsR: a new R package for data handling and analysis in
732 macroecology. Methods in Ecology and Evolution, 6, 1229–1234.
733 Wickham, H. (2016). ggplot2: Elegant Graphics for Data Analysis. New York: Springer-Verlag
734 New York. http://ggplot2.org
735 Yu, G. (2019). treeio: Base Classes and Functions for Phylogenetic Tree Input and Output. R
736 package version 1.6.2. https://guangchuangyu.github.io/software/treeio

737 Yu, G., Smith, D., Zhu, H., Guan T., & Lam, T. T-Y. (2017). ggtree: an R package for
738 visualization and annotation of phylogenetic trees with their covariates and other associated
739 data. Methods in Ecology and Evolution, 8, 28–36.

740 **FIGURES**

741 **Figure 1.** Relationship between tail length and climatic variables. (a) Example of one of the 100
742 completed phylogenetic trees used in the phylogenetic regressions, with branch colors
743 corresponding to the maximum likelihood estimates of the ancestral states for tail length. (b)
744 Map of assemblage-level mean tail length (log-transformed) values shown at 10 arc-min
745 resolution (note that we aggregated to 1.5-degree grid cells for all assemblage-based analyses).
746 (c) Mean AICc weight of models including each bioclimatic variable or none (i.e. null model) (d)
747 Standardized effect sizes based on coefficient estimates ($\beta$) ± 95% confidence intervals (CI) for
748 the regression between tail length and the climate variables at the level of species (left,
749 phylogenetic regressions) or assemblages (right, spatial regressions). Results shown in (e) are the
750 effect of the interaction between climate [i.e. the climate variable with the highest AICc weight
751 as shown in (c); results are thus averaged across the subset of models for which this variable was
752 selected] and two interacting continuous variables: range size and body size (top), as well as the
753 estimated marginal slope of the relationship between tail length and climate for each level of
754 three interacting factor variables: habitat type, life mode, and saltation ability (bottom). All
755 confidence intervals are drawn from the distribution of coefficient estimates across the 100
756 repetition of random sampling, and additionally across 100 phylogenetic trees for both the DNA-
757 only trees and the completed trees in which DNA-missing species were imputed. Tail length
758 across assemblages was summarized by either the median, the $10^{th}$ or the $90^{th}$ percentile value.
759 Climatic variables are defined as follows: BIO1=annual mean temperature, BIO5=maximum
760 temperature of the warmest month, BIO6=minimum temperature of the coldest month,
761 BIO12=annual precipitation, BIO13=precipitation of the wettest month, BIO14=precipitation of
762 the driest month. Results are also reported in Tables S4, S5, and S6. Silhouettes were
763 downloaded from publicdomainpictures.net.

764

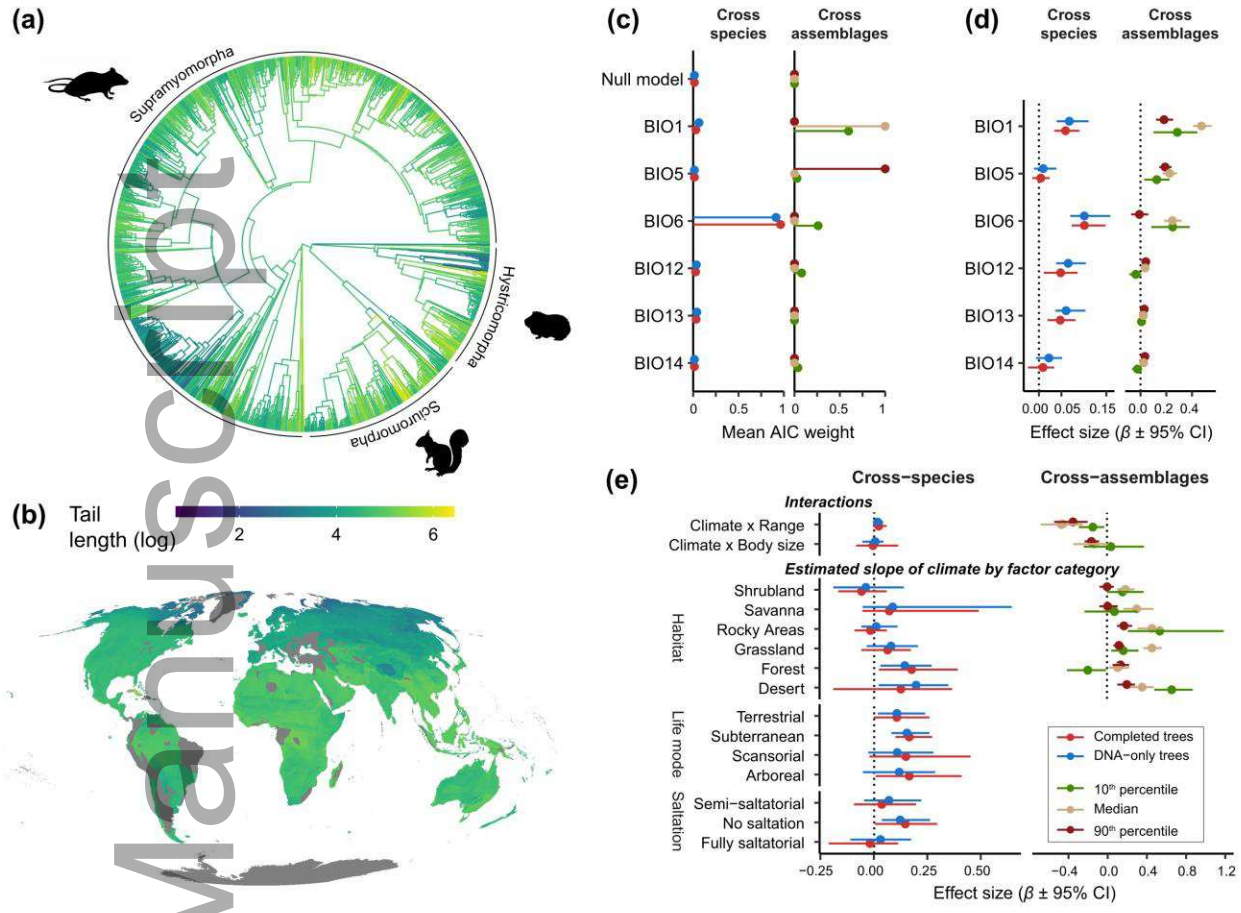


765
766

767 **Figure 2.** Relationship between hind foot length and climatic variables. (a) One of the 100
768 phylogenetic trees used in the phylogenetic regressions, with branch colors corresponding to the
769 maximum likelihood estimates of the ancestral states for hind foot length. (b) Map of
770 assemblage-level mean hind foot length (log-transformed) values shown at 10 arc-min resolution
771 (assemblage-based analyses were performed in 1.5-degree grid cells). (c) Mean AICc weight of
772 models including each bioclimatic variable or none (i.e. null model). (d) Standardized effect
773 sizes based on coefficient estimates (ß) ± 95% confidence intervals (CI) for the regressions
774 between hind foot length and the climate variables. (e) Interaction between the selected climate
775 variable and species characteristics. See the Figure 1 legend for more information.

776

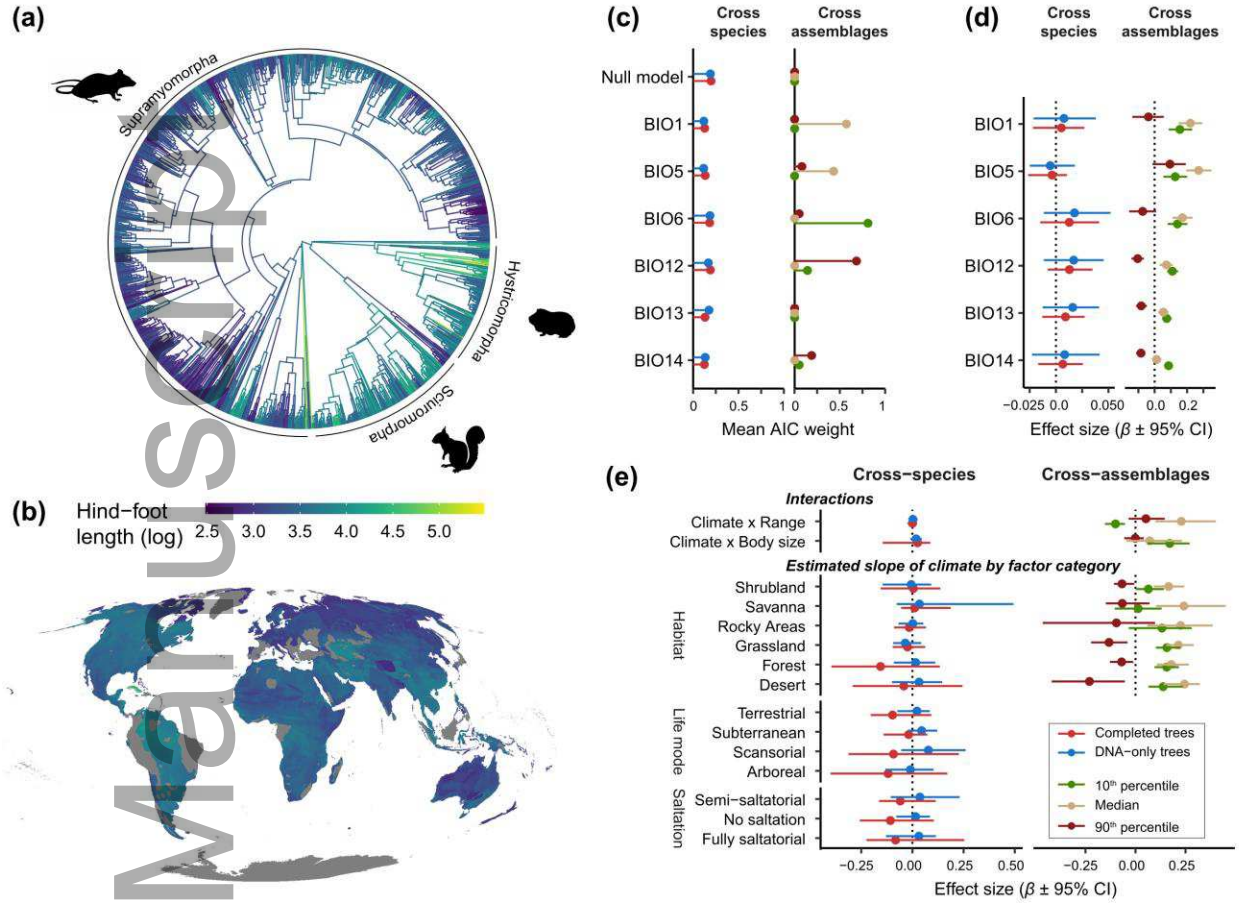


777
778

779 **Figure 3.** Relationship between ear length and the climatic variables. (a) One of the 100
780 phylogenetic trees used in the phylogenetic regressions, with branch colors corresponding to the
781 maximum likelihood estimates of the ancestral states for ear length. (b) Map of assemblage-level
782 mean ear length (log-transformed) values shown at 10 arc-min resolution (assemblage-based
783 analyses were performed in 1.5-degree grid cells). (c) Mean AICc weight of models including
784 each bioclimatic variable or none (i.e. null model). (d) Standardized effect sizes based on
785 coefficient estimates (ß) ± 95% confidence intervals (CI) for the regressions between ear length
786 and the climate variables. (e) Interaction between the selected climate variable and species
787 characteristics. See the Figure 1 legend for more information.

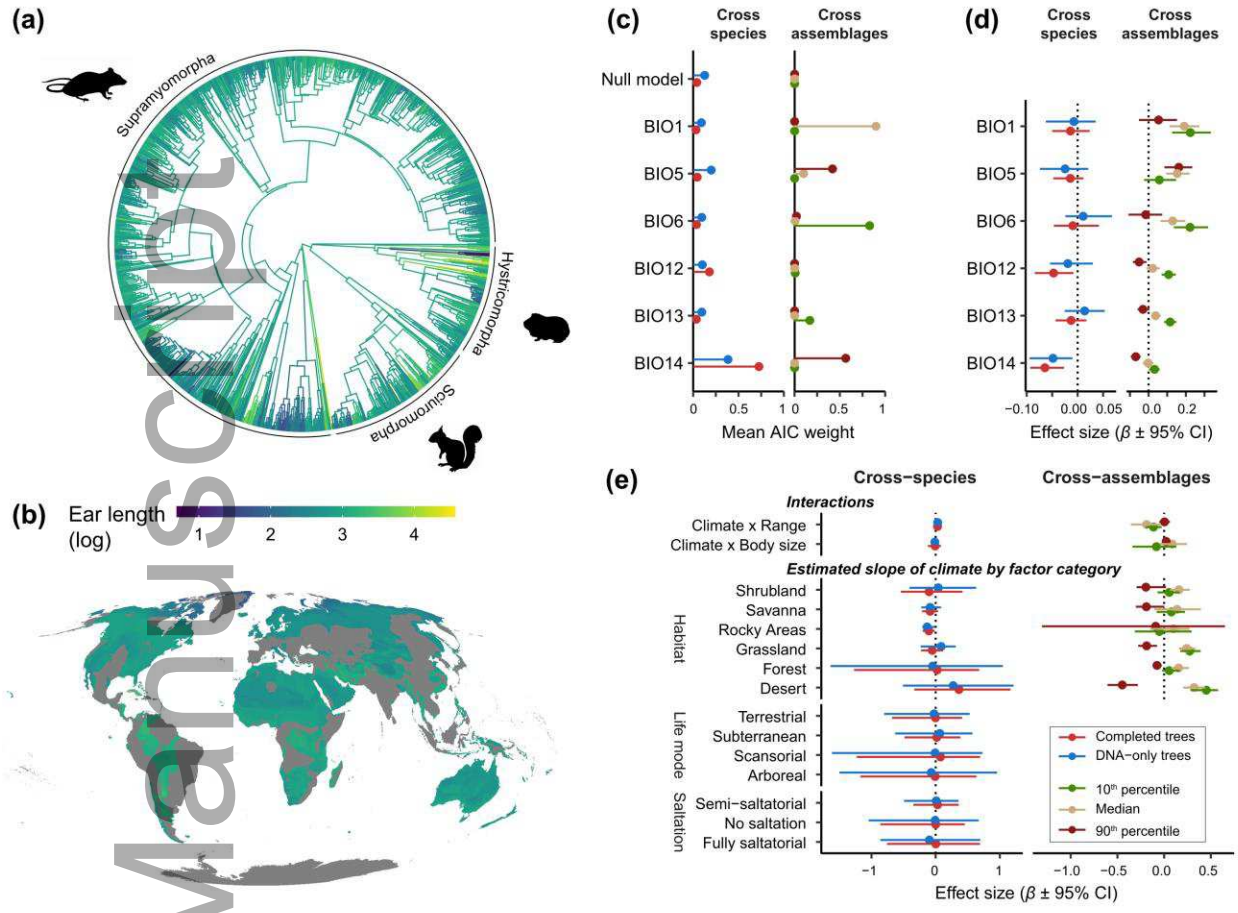


788

789

790 **SUPPORTING INFORMATION**

791 **Appendix S1.** Morphometric data collection, processing, cleanup, quality control, and
792 preliminary analyses (supplementary methods).

793 **Appendix S2.** R script used to perform the phylogenetic and spatial regression analyses.

794 **Table S1.** Morphometric data retrieved from museum databases and the literature. The
795 descriptions of the columns and the abbreviations for the collections appear in the "Metadata"
796 sheet. The references appear in the "References" sheet. Observations (rows) lacking head and
797 body length and at least one appendage length (tail length, hind foot length, ear length) were not
798 included in this data set and thus are not used in any of the analyses. All data are untransformed.
799 Blank cells indicate missing data.

800 **Table S2.** Species means for morphometric and environmental data, along with habitat, life
801 mode, and saltation ability. Species means of morphometric data were calculated based on the

data shown in Table S1. The descriptions of the columns appear in the "Metadata" sheet. Species with environmental data only (no morphometric data) were not included in this data set and thus are not used in any of the analyses. All data are untransformed. Blank cells indicate missing data.

**Table S3.** List of species in Table S2 that are not found in the Upham et al. (2019) phylogeny, and their synonyms, when available. Blank cells indicate species with no matching synonyms in the Upham et al. (2019) phylogeny. See the "Metadata" sheet for more details.

**Table S4.** Results of the relationship between appendage length and the absolute value of latitude.

**Table S5.** Results of the relationship between appendage length and climate.

**Table S6.** Proportion of significant interactions between climate and habitat, body size, range size, life mode, and saltation.

**Figure S1.** Relationship between appendage length and latitude (absolute value). Standardized effect sizes are represented as coefficient estimates (ß) ± 95% confidence intervals (CI) for the regressions between tail length, hind foot length, and ear length and the absolute value of latitude, for the cross-species analyses and for the cross-assemblage analyses. Results are based on 100 repetitions of random sampling and, for cross-species analyses, 100 phylogenetic trees. Climatic variables are defined as follows: BIO1=annual mean temperature, BIO5=maximum temperature of the warmest month, BIO6=minimum temperature of the coldest month, BIO12=annual precipitation, BIO13=precipitation of the wettest month, BIO14=precipitation of the driest month.

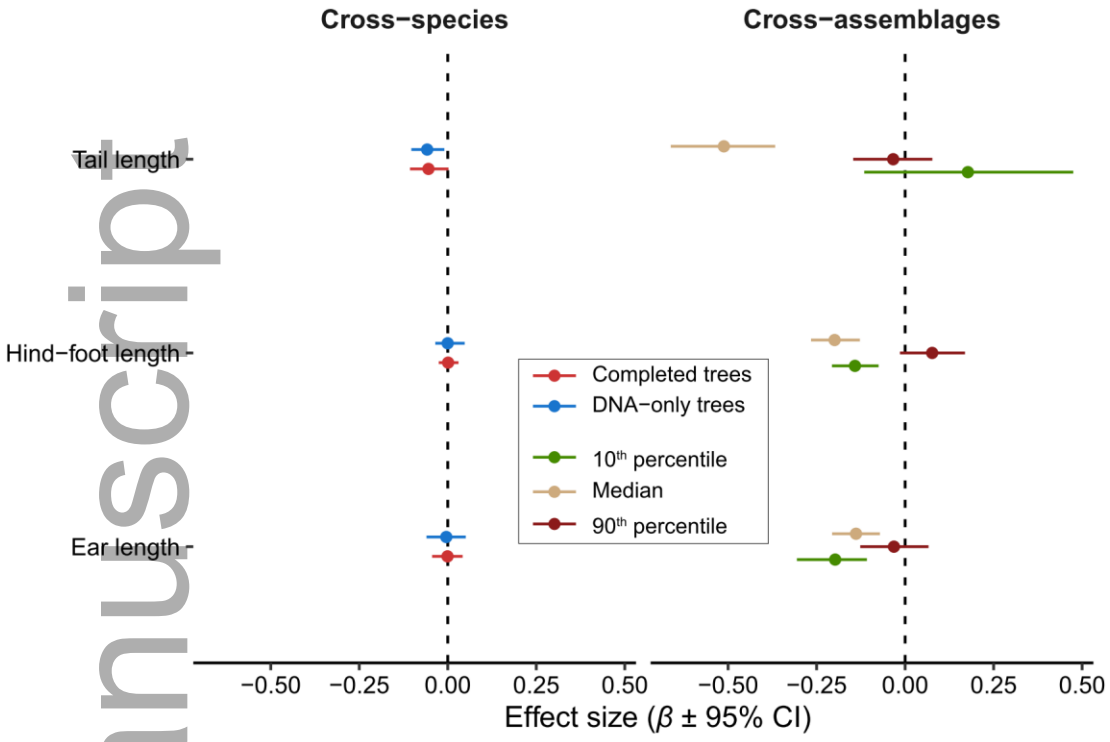


822